Nematic-isotropic phase transition in a liquid-crystal droplet

S. Kralj
J. Stefan Institute, University of Ljubljana, Jamova 39, 61111 Ljubljana, Yugoslavia

S. Žumer
Liquid Crystal Institute and Department of Physics, Kent State University, Kent, Ohio 44242, and J. Stefan Institute and Physics Department, University of Ljubljana, 61111 Ljubljana, Yugoslavia

D. W. Allender
Liquid Crystal Institute and Department of Physics, Kent State University, Kent, Ohio 44242
(Received 15 August 1990)

Possible phases in a nematic liquid crystal confined to a spherical submicrometer droplet embedded in a solid polymer are analyzed in terms of a Landau–de Gennes theory. For a droplet with a radial structure we show that the strength of the nematic-polymer interfacial interaction affects the nematic-paranematic (partially ordered isotropic phase) phase transition and may in addition induce a boundary-layer nematic phase. This boundary layer phase exists only in a narrow (~ 0.1 K) temperature interval above the nematic phase for a restricted range of interfacial interactions. Also in the radial structure the degree of ordering is suppressed close to the center of the droplet where a defect is located. As the size of the droplet decreases, the relative size of this region of suppressed ordering increases. Below a critical radius R_c (0.22 μm for 4-*n*-pentyl-4'-cyanobiphenyl), if the surface interaction is above a critical value ($q_{\max}=1.85\times 10^{-3}$), the transition between the nematic phase and the paranematic phase no longer occurs. A three-dimensional phase diagram is presented to demonstrate the effect of the surface interaction strength, droplet radius, and sample temperature on the stability of phases within a droplet.

I. INTRODUCTION

There has been considerable interest over the past few years in geometrically confined systems and related surface phenomena. In the field of liquid crystals such systems are of interest due to their importance in the electro-optic industry. Studies of a liquid crystal confined to small droplets have been stimulated recently by the appearance of a new generation of liquid-crystal shutters and displays based on the use of polymer-dispersed liquid crystals[1–3] (PDLC). These materials are dispersions of micrometer-size liquid-crystal droplets embedded in a solid polymer matrix. Droplets with a relatively small variance in radius are formed during the polymerization process of the liquid-crystal–polymer (epoxy resin) mixture. The average droplet radius varies from the submicrometer region up to 100 μm, depending on the conditions that regulate the polymerization process. Due to a high surface-to-volume ratio in PDLC, surface interactions strongly influence the structure within droplets. Structures of such droplets are characterized by specific orientational and positional ordering. The latter is present only in phases where smectic ordering appears. Here we limit our discussion to a system where a nematic or a very weakly nematic (paranematic) ordering is present. In such systems a structure is characterized by the positional dependence of the nematic order parameter which is a second rank tensor. If the ordering is uniaxial the structure is completely described by the director field (configuration) and the positional dependence of the scalar order parameter S.

The types of structures commonly reported depend on the boundary condition for the director at the surface. For homeotropic anchoring at the polymer-nematic interface the radial and axial configurations are seen; and bipolar, twisted bipolar, and concentric configurations occur for tangential anchoring, where the nematic director is parallel to the droplet surface. In the radial configuration[4,5] [Fig. 1(a)] the nematic director field emerges radially from the central point defect. This configuration is stable in the strong homeotropic anchoring regime. An external field deforms the structure or even shifts the point defect toward the surface.[6–8] If the anchoring is weak or if there is a strong external field the axial configuration[6–9] is stable. In the axial configuration the largest elastic deformations appear close to the equator of the droplet. Depending on the strength of the external field and anchoring the structure can be defectless [Fig. 1(b)] or have a concentric line defect in the equatorial plane[6,9] [Fig. 1(c)]. In the bipolar configuration[4,5] [Fig. 1(d)], which is stable for parallel surface anchoring if the three Frank elastic constants are comparable, nematic director field lines resemble the electric field between two charges of the opposite sign. They connect the two opposite poles of the droplet lying on the axis of the droplet. If the value of the twist elastic constant is low the twisted bipolar[10] [Fig. 1(e)] configuration appears. There the nematic director field

rotates around the droplet axis. In the case of a very low ratio of the bend to splay elastic constants the toroidal configuration[11] [Fig. 1(f)] is stable. It has concentric nematic director lines with a line defect along the symmetry axis. The existence of some of these configurations has been confirmed experimentally by microscopic observations[5,12] in supramicrometer droplets and using deuterium NMR (Refs. 13 and 14) and a light-scattering study[15] in submicrometer nematic droplets.

Most of the work probing the spatial dependence of the order parameter has been for the case of a liquid crystal in contact with a solid planar surface. These studies show that because of the interfacial interactions liquid-crystal molecules close to the surface exhibit some nematic order even at temperatures corresponding to the isotropic phase in a bulk liquid crystal.[15–30] Such a partially ordered state is usually called the "paranematic" phase. In addition, Sheng[19] predicted, using the Landau–de Gennes approach, the existence of a first-order boundary-layer transition (orientational prewetting transition) at which the nematic order in a boundary layer much thicker than the coherence length is discontinuously increased. This transition may appear only for a restricted range of surface interaction potential strengths near the transition (~ 0.1 K) into the bulk nematic phase. Sheng also demonstrated that decreased enclosure size shifts the nematic-paranematic transition towards higher temperatures, and at a critical size the transition is replaced by a continuous development of nematic order. Poniewierski and Sluckin[20] studied the same system with a Maier-Saupe model and obtained only qualitative accordance with the results of Sheng. Also some experimental studies have been devoted to the effect of the surface on the nematic ordering close to the nematic-isotropic transition. The orientational wetting of planar surfaces has been studied by evanescent-wave ellipsometry.[24,25] The transition-temperature shift in planar films of varying thickness has been verified by birefringence measurements.[26] Preliminary theoretical studies[27–29] have shown that in a nematic (5CB) droplet the critical droplet radius, where the nematic-paranematic transition becomes continuous, is $R_c \sim 0.16$ μm in droplets with the radial structure and $R_c \sim 0.07$ μm in droplets with the bipolar structure. The first experimental evidence of this phenomenon in droplets has been demonstrated using deuterium NMR in PDLC.[30] The existence of the surface layer transition has not yet been experimentally verified.

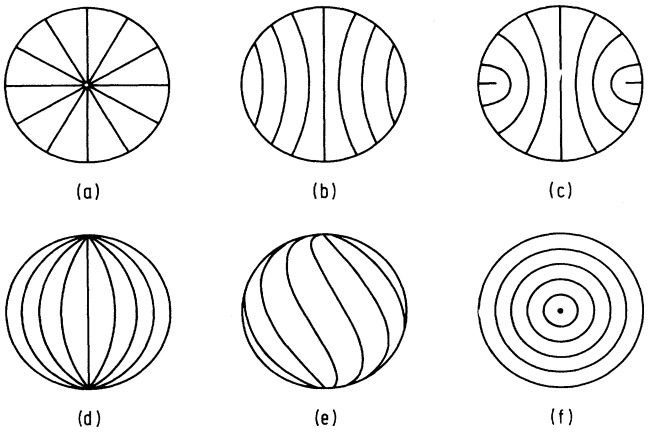

FIG. 1. A schematic representation of the most common structures in a nematic droplet: (a) radial, (b) axial, and (c) axial with a line defect, in the case of homeotropic anchoring; and (d) bipolar, (e) twisted bipolar, and (f) concentric structure, which appear for tangential anchoring at the polymer-nematic interface.

In this contribution we study the influence of the confinement on the degree of the nematic ordering in a droplet of a nematic liquid crystal. To simplify calculations we limit our treatment to a spherical droplet where a strong homeotropic anchoring induces a radial configuration in the nematic phase. The results are expected to be at least qualitatively relevant also for more general cases. In Sec. II we use the Landau–de Gennes phenomenological approach and an approximate surface interaction contribution having a term linear in the nematic order parameter. We discuss the stability of possible phases with respect to changes in the surface interaction, droplet radius, and sample temperature in Sec. III. Special attention is paid to the neighborhood of the nematic-paranematic phase transition where the boundary-layer nematic phase transition may appear at an appropriate strength of the surface interaction. The results are summarized in a phase stability diagram.

II. LANDAU–de GENNES FREE ENERGY

In order to have a simple radial ordering in the nematic droplet we limit our discussion to cases where a strong homeotropic anchoring is enforced at the spherical droplet surface. The nematic director $\mathbf{n}$ is radial everywhere. There is only a splay-type elastic deformation, and the symmetry of the local director fluctuations is not broken. Therefore uniaxial ordering is expected. This, together with the fact that the radial director field does not change, enables us to completely describe the phase in such a droplet by a single scalar order parameter. The local value of the orientational order parameter $S(r)$ is given by $S(r)=\langle 3\cos^2\theta-1\rangle/2$, with θ being the angle between the average and instantaneous direction of nematic director $\mathbf{n}$ at a point $\mathbf{r}$ and $\langle\ \rangle$ indicating time average.[31]

To find the possible phases we minimize the Landau–de Gennes free-energy density $f(r)$, which in the absence of an external magnetic or electric field can be written as a sum of a surface interaction term f_s and two bulk terms: f_h, which does not vanish in the homogeneous phase; and f_d, which is different from zero only in a nonhomogeneous phase. For f_h we use the well-known expansion in terms of the powers of the order parameter:[32]

$$f_h = f_0(T) + a\Delta T\frac{S^2}{2} - b\frac{S^3}{3} + c\frac{S^4}{4}\ , \tag{1a}$$

where f_0 is the free energy of the isotropic phase and a, b, and c are the Landau phenomenological material con-

stants, which can be determined by comparison with experiments. Instead of the absolute temperature T, we use the temperature $\Delta T = T - T_*$ which is measured relative to T_*—the temperature of the supercooling limit.

Following Sheng[32] the f_d term, which includes the lowest allowed powers of the derivatives of the director field and order parameter, can be written as

$$f_d = \tfrac{3}{4} L_1 (\nabla S)^2 + \tfrac{9}{4} L_1 S^2 [(\nabla \cdot \mathbf{n})^2 + (\nabla \times \mathbf{n})^2] \ . \quad (1b)$$

Here we use a single elastic constant approximation (corresponding to $L_2 = 0$ in Ref. 32), where L_1 is a temperature-independent constant. According to the assumption of strong anchoring the molecules are on the average oriented along the easy direction at the nematic-polymer interface so that the surface interaction depends only on the degree of orientational order.[33] Following Sheng,[19] we use the simplest form of the f_s term:

$$f_s = -GS\delta(r - R) \ . \quad (1c)$$

Here G is a a surface coupling, R the droplet radius, and $\delta(r - R)$ a delta function.

For the case of the radial configuration within the spherical droplet, the free-energy density can be written in terms of a dimensionless spherical coordinate $\rho = r/R$ and dimensionless constants $A = \frac{2}{9}(R/\xi_0)^2$, $C = cR^2(2/9L_1)$, $B = bR^2(2/9L_1)$, $q = \frac{2}{9}(G/\sqrt{aL_1 T_*})$, $\lambda = R/\xi_0$, where $\xi_0 = [L_1/(aT_*)]^{1/2}$ is the zero-temperature coherence length:

$$f(r) - f_0(T) = \frac{9}{2}\frac{L_1}{R^2}\left[\left[\frac{A}{2}\frac{\Delta T}{T_*} + \frac{2}{\rho^2}\right]S^2 - \frac{BS^3}{3} + \frac{CS^4}{4} + \frac{1}{6}\left[\frac{\partial S}{\partial \rho}\right]^2 - q\lambda S\delta(1-\rho)\right] . \quad (2)$$

The minimization of the free-energy functional $F([S(r)]) = \int f(r) d^3\mathbf{r}$ leads to the following differential equation:

$$\frac{\partial^2 S}{\partial \rho^2} + \frac{2}{\rho}\frac{\partial S}{\partial \rho} - 3\left[\left[A\frac{\Delta T}{T_*} + \frac{4}{\rho^2}\right]S - BS^2 + CS^3\right] = 0 \ , \quad (3)$$

which must be solved to get the positionally dependent order parameter $S(\rho)$. In the center of the droplet ($\rho = 0$) there is always a defect, so the solution must satisfy the condition $S(\rho = 0) = 0$. On the outer surface the minimization of the free energy with a variable end point [i.e., $S(\rho = 1)$ is a variable] leads to the boundary condition $(\partial S/\partial \rho)_{\rho=1} = 3q\lambda$. Results obtained for various cases are discussed in the following section.

III. RESULTS

In the first step the partial differential equation (3) is solved numerically using the relaxation method for a chosen surface order parameter value $S(r = R)$. In the second step the surface free-energy term is taken into account and the equilibrium value $S(r = R) = S_0$ is obtained after the minimization of the total free energy. In the calculations we used parameters characteristic of the common nematic liquid crystal 5CB [$a = 0.1319 \times 10^6$ J/(m^3 K), $b = 1.836 \times 10^6$ J/m^3, $c = 4.050 \times 10^6$ J/m^3, $L_1 = 6 \times 10^{-12}$ J/m, and $T_* = 307$ K, which is 1.402 K below the bulk transition temperature]. In Fig. 2 structures for three different temperatures in a droplet of radius $R = 0.4$ μm are presented. The bars indicate the director field and the length of the bars is proportional to the local value of $S(r)$. We see that the ordering is always nonuniform, and therefore there is no longer a clear

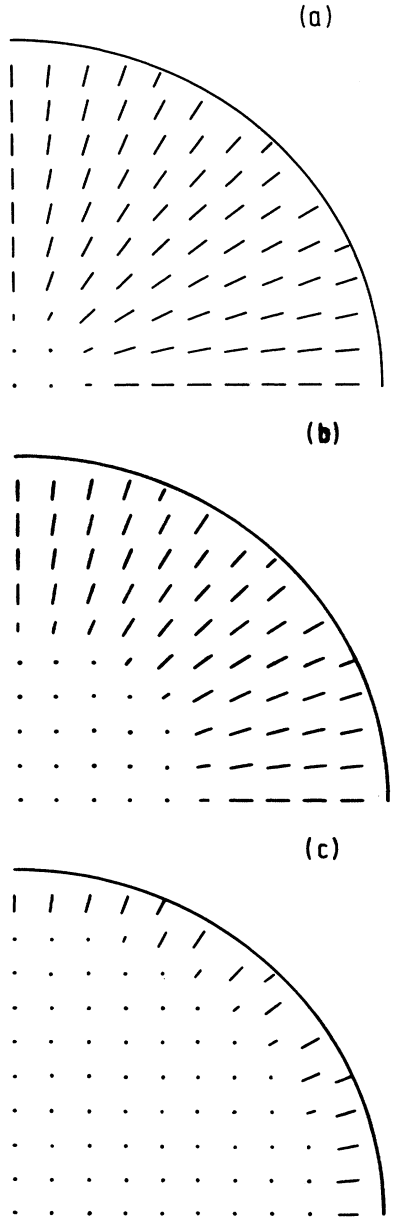

FIG. 2. Computer simulation of the radial structure in a spherical droplet with radius $R = 0.4$ μm in a nematic phase [(a) $\Delta T \sim 1.30$ K, (b) $\Delta T \sim 1.415$ K] and in a boundary layer nematic phase [(c) $\Delta T \sim 1.415$ K]. The length of the bars is proportional to the local order parameter.

distinction between the ordered and disordered phases, unlike the bulk case. In the following the term paranematic (P) will be used for the phases where there is only a thin weakly ordered [$S_0 \ll S_{\text{bulk}} = 4b/(3c)$] boundary layer. The term nematic (N) will be used for the phase where $S(r) \sim \text{const} \sim S_{\text{bulk}}$ in a substantial part of the droplet. The term boundary-layer nematic phase (N_{BL}) will stand for a phase where a major part of the droplet is in the isotropic phase but where there is a strongly ordered boundary layer [S (boundary layer) $\sim S_{\text{bulk}}$].

Let us first examine droplets with relatively large radius ($R = 1\ \mu\text{m} \sim 2600\xi_0$) so that the effect of the defect is small. In Figs. 3(a) and 3(b) the temperature dependence of the surface order parameter S_0 is compared with $\bar{S}$, which is defined by averaging $S(r)$ over the whole droplet. The different curves correspond to different strengths of the surface interaction where the dimensionless parameter q ranges from zero to 2.1×10^{-3}. It is obvious that for any finite q value, nematic molecules at the droplet surface are partially ordered also at relatively high temperatures, corresponding to the isotropic phase in the bulk case. According to our definition this is a paranematic phase. With decreasing temperature at relatively low surface interaction strength ($q < 0.85 \times 10^{-3}$), the paranematic phase at the transition temperature $T_n(q,R)$ discontinuously transforms into the nematic phase. The first-order transition is manifested by a jump in S_0 and $\bar{S}$ values, indicating sudden ordering both in the droplet interior and on the droplet surface. This transition temperature weakly increases with increasing q. For surface interactions with $q > q_{\min}(R) \sim 0.85 \times 10^{-3}$ the surface coupling is strong enough to induce the appearance of a boundary-layer nematic phase (N_{BL}), which is manifested by an additional discontinuous change in ordering of molecules in a surface layer relatively thick compared to ξ_0. This first-order orientational prewetting transition occurs at $T_s(q,R)$, which is slightly above the temperature of the transition into the nematic phase T_n so that the N_{BL} phase is stable only in a narrow tempera-

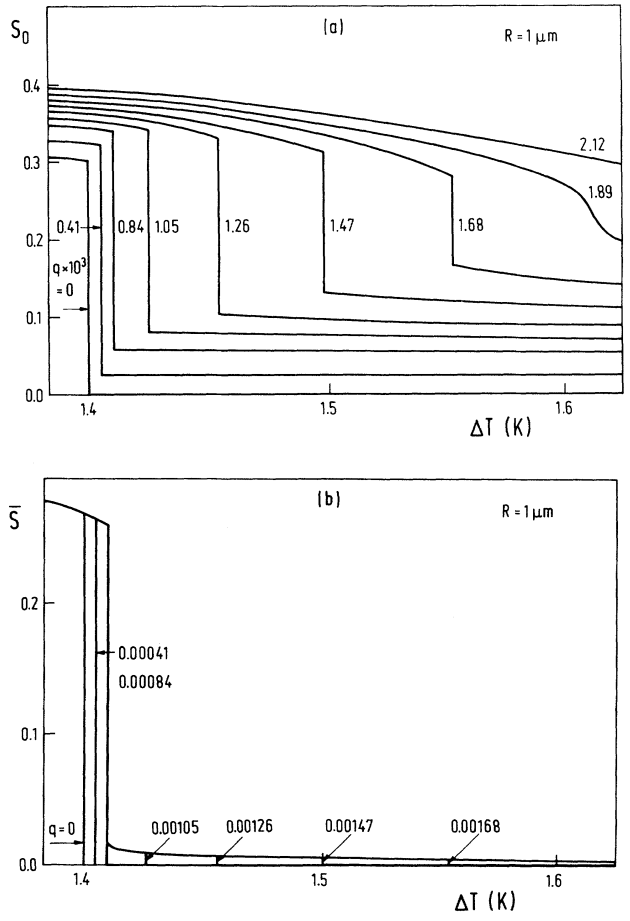

FIG. 3. (a) Calculated order parameter S_0 at the polymer-nematic interface and (b) the average order parameter $\bar{S}$ plotted as functions of temperature for different surface interactions and $R = 1\ \mu\text{m}$. The simultaneous jump in $\bar{S}$ and S_0 reflects a transition from a paranematic to a nematic phase, and a jump visible only in S_0 indicates a transition from a paranematic to an N_{BL} phase.

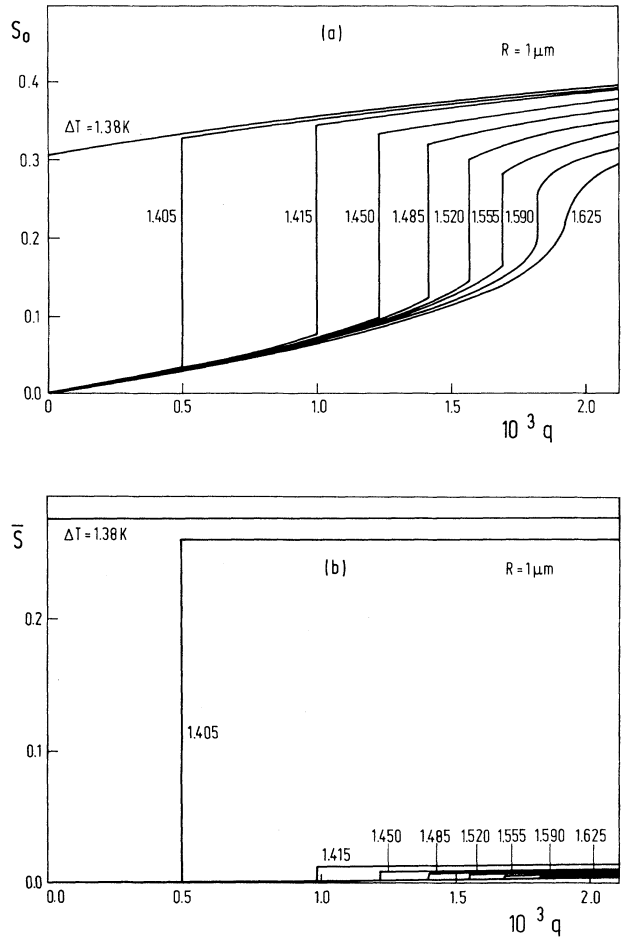

FIG. 4. (a) S_0 and (b) $\bar{S}$ as functions of the surface interaction at different sample temperatures in a droplet with a radius 1 μm well above the critical value $R_c \sim 0.22\ \mu\text{m}$.

ture interval (<0.1 K, depending on the liquid-crystal material and the surface interaction strength). It is accompanied by a substantial jump in the surface ordering S_0 [Fig. 3(a)], while $\bar{S}$ [Fig. 3(b)] is only weakly influenced because the ordered boundary layer consists of only a small fraction of the volume of the droplet. With increasing q the transition temperature $T_s(q,R)$ slightly shifts towards higher values. For even stronger surface interaction with $q > q_{\max}(R) \sim 1.9\times10^{-3}$ the surface coupling dominates the ordering close to the surface. The order in the surface layer changes continuously with temperature and the distinction between the paranematic phase and the N_{BL} phase disappears. The P-N_{BL} transition line ends in a critical point at $q_{\max}(R)$. As will be discussed later, $q_{\min}(R)$ and $q_{\max}(R)$ are nearly constant for all $R > 0.22$ μm.

In Figs. 4(a) and 4(b) the changes of the ordering within an $R = 1$-μm droplet as a function of the surface interaction q are illustrated by the functions $\bar{S}(q)$ and $S_0(q)$. The various curves correspond to different values of ΔT. At $T = 1.38$ K the droplet is in the nematic phase for all q. With increasing surface interaction the ordering of molecules near the droplet surface is continuously increasing [Fig. 4(a)], while the ordering within the droplet is only weakly influenced [Fig. 4(b)]. At $\Delta T = 1.405$ K the droplet is in the paranematic phase at small-q values but the temperature is still low enough for the nematic phase to occur at higher surface interactions. For temperatures above $\Delta T \sim 1.415$ K the nematic phase is not stable anymore. In the temperature interval 1.415 K $< \Delta T < 1.6$ K, as q increases there is a P to N_{BL} transition. At still higher temperatures only the P phase is stable.

In Fig. 5 the spatial variation of the order parameter within a droplet above and below the N-N_{BL} and N_{BL}-P phase transitions is shown. For a droplet radius $R = 0.4$ μm $\sim 1040\xi_0$ and the surface interaction strength $q_{\min}(R) < q = 1.5\times10^{-3} < q_{\max}(R)$, both transitions occur and the thickness of the surface layer is $\sim R/10$. The N-N_{BL} transition is at $\Delta T = 1.415$ K and the N_{BL}-P transition at $\Delta T = 1.510$ K.

At small radii the ordering in most parts of the droplet is affected either by the elastic deformations or by the surface interaction. At a critical radius $R = R_c \sim 0.22$ μm $\sim 570\xi_0$ and $q > q_{\min}(R_c)$ the transition from the nematic phase to the N_{BL} phase becomes continuous (i.e., the N and N_{BL} phases become identical) and below R_c there is no longer an N-N_{BL} transition. An example of this is evident from the temperature dependence of S_0 and $\bar{S}$ [Figs. 6(a) and 6(b)] for different values of q in a droplet with $R = 0.1$ μm $\sim 260\xi_0$. At large $q > q_{\max}(R) \sim 1.7\times10^{-3}$, the three phases are indistinguishable. No transitions occur. The order simply increases smoothly as ΔT decreases. Below $q_{\max}(R)$ the transition between the P phase and the N_{BL} phase at T_s is

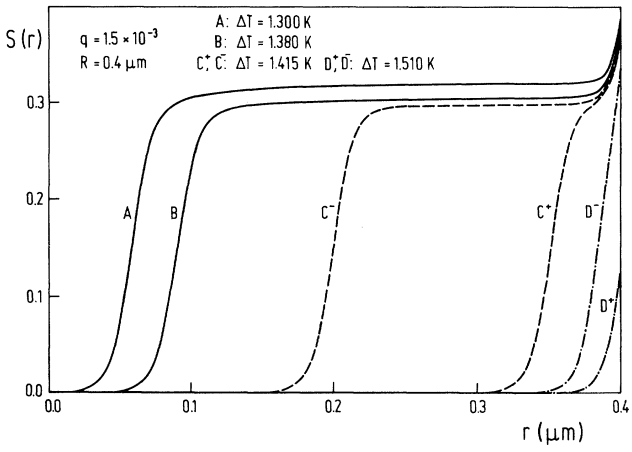

FIG. 5. Spatial variation of the order parameter within a spherical droplet of a radius $R = 0.4$ μm and surface interaction $q \sim 1.5\times10^{-3}$. Curves A, B, and C^- correspond to the N phase, C^+ and D^- to the N_{BL} phase, and D^+ to the P phase. Cases C correspond to describe the N-N_{BL} transition and cases D to describe the N_{BL}-P transition.

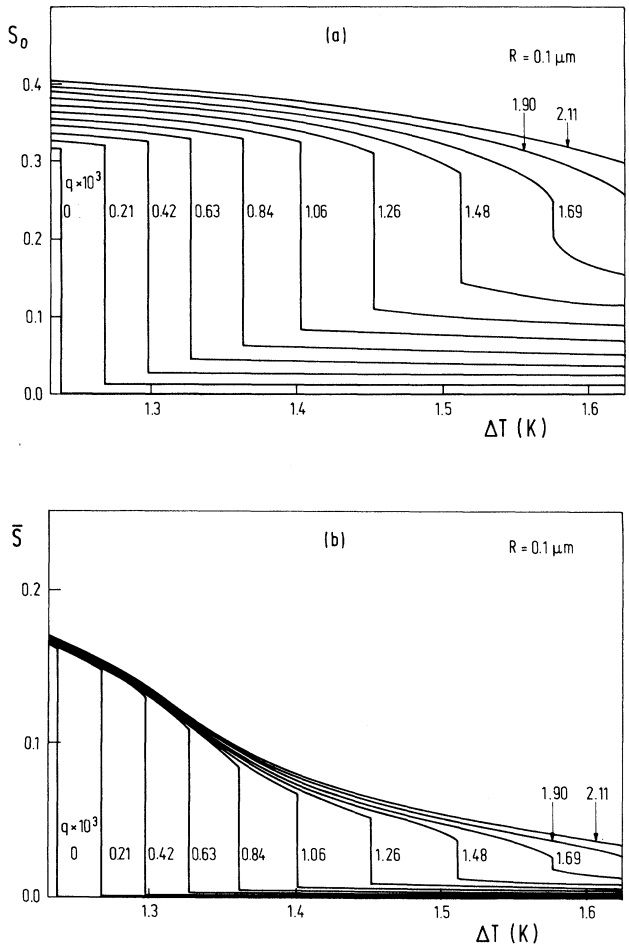

FIG. 6. (a) Surface ordering and (b) average parameter $\bar{S}$ as functions of temperature for various surface interactions in a droplet with radius 0.1 μm well below the critical value $R_c \sim 0.22$ μm.

discontinuous, but the N_{BL} and N phases are indistinguishable and no further transition occurs. The jump in $\bar{S}$ is even larger than at $R=1\ \mu m \sim 2600\xi_0$, since in smaller droplets there is a larger relative amount of molecules in the ordered surface layer. This is evident from the spatial dependence of the order parameter below and above the $q_{max}(R)$ shown in Figs. 7(a) and 7(b). In Figs. 8(a) and 8(b) the effect of the surface boundary-layer nematic-paranematic transition on the discontinuity of S_0 and $\bar{S}$ in small droplets is shown.

IV. DISCUSSION

The results described above are summarized in the temperature-surface interaction-radius phase diagram (Fig. 9) presenting stability regions of the paranematic, nematic, and boundary-layer nematic phases. The phases are separated by "transition surfaces." The N-N_{BL} surface terminates at small R in a line of critical points R_c, where the distinction between the two phases vanishes. At small q the N-N_{BL} surface merges in a line of triple points $q_{min}(R)$, with the P-N_{BL} surface and the P-N surface. The P-N_{BL} surface terminates at large q in a line of critical points, q_{max}, where again the distinction between the corresponding phases vanishes. Regions of small q's and R's, where our strong anchoring assumption is particularly unrealistic are not shown. More attention is paid to the area close to the triple line, which is presented in Fig. 10 in detail where a projection of the three-dimensional phase diagram on the temperature-surface interaction plane is drawn. The projections of the line of triple points q_{min} and of the two critical lines q_{max} and R_c on the temperature-radius and the surface interaction-radius planes are shown in Figs. 11(a) and 11(b). The line of critical points R_c is practically parallel to the q axis and the line of triple points is practically parallel to the R axis, while the q_{max} curve is nearly parallel to the q axis for small radii ($\ll R_c$) but nearly parallel to the R axis for $R > R_c$.

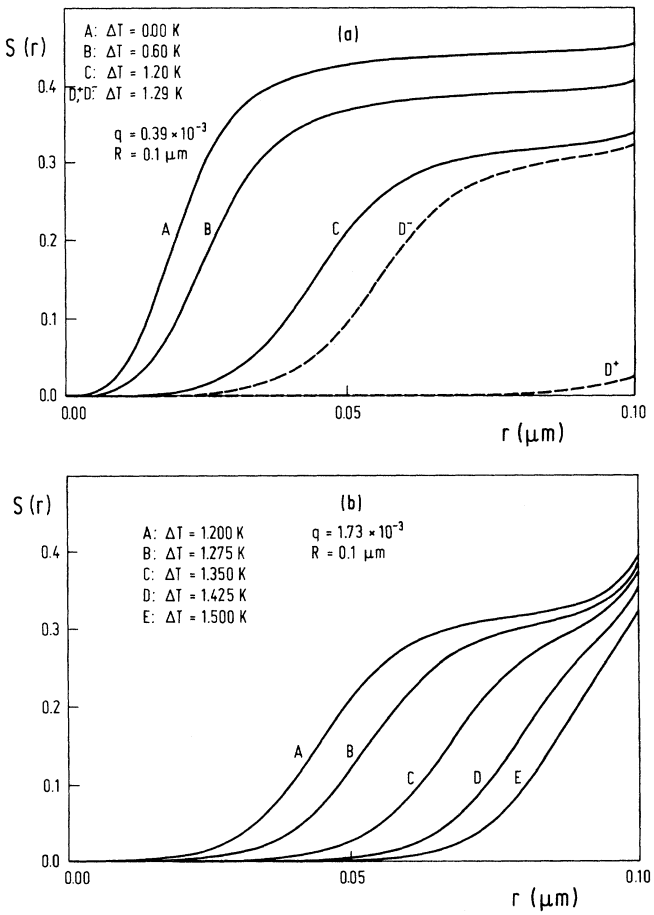

FIG. 7. Variation of the order parameter $S(r)$ in a droplet with radius well below the critical value R_c at different temperatures and surface interactions: (a) $q \sim 0.4\times10^{-3} < q_{max}$ and (b) $q \sim 1.7\times10^{-3} > q_{max}$. In (a) curves A and B correspond to the N phase, C and D^- to the N_{BL} phase, and D^+ to the P phase. Cases D demonstrate the N_{BL}-P transition. The N_{BL} and N phases are indistinguishable. In (b) all phases are indistinguishable.

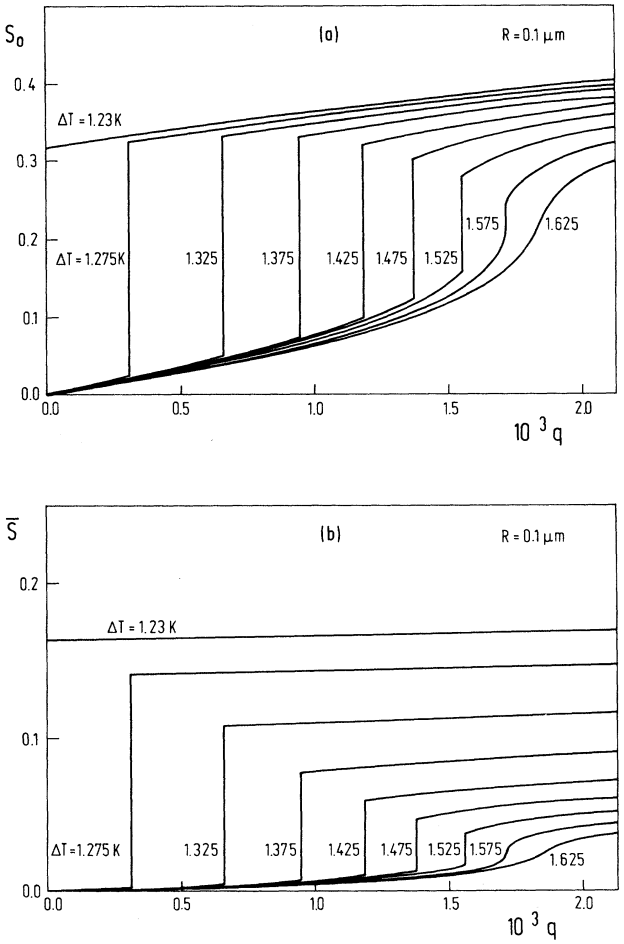

FIG. 8. Variation of (a) S_0 and (b) $\bar{S}$ with the surface interaction at different temperatures. The droplet radius is 0.1 μm, which is below the critical value $R_c \sim 0.22\ \mu m$.

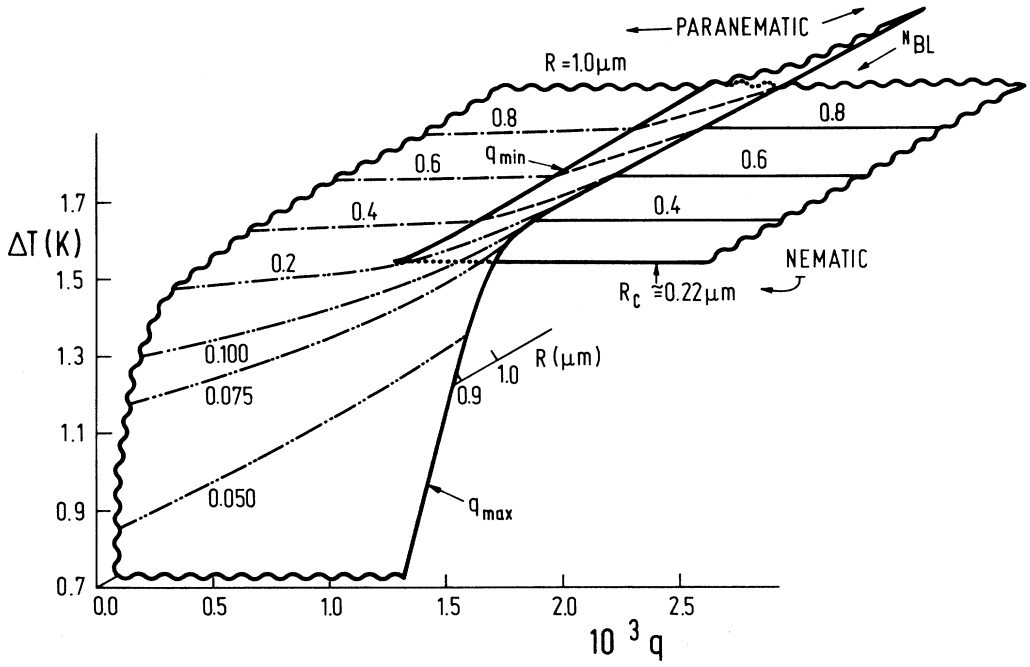

FIG. 9. Three-dimensional phase diagram of a nematic liquid crystal confined to a spherical droplet as a function of the surface interaction, droplet radius, and sample temperature. All "transition surfaces" correspond to first-order transitions. The lines of constant radii in each transition surface indicates its nature: lines marked (—·—·—·) are in the P-N transition surface, lines marked (——) are in the N_{BL}-N transition surface, lines denoted (— — —) make up the P-N_{BL} transition surface for droplet radii $R > R_c \sim 0.22$ μm, and the lines marked (–···–··–) give the P-N_{BL} transition surface for droplet radii $R < R_c$.

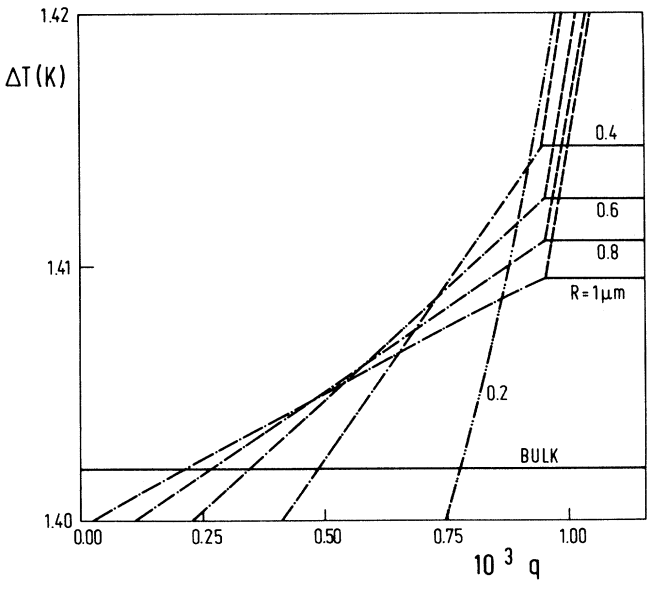

FIG. 10. For several droplet radii the projections of the stability regions on the temperature-surface interaction plane are shown close to the triple point. The reference line at $\Delta T \sim 1.402$ K indicates the bulk nematic transition. The following notation is used: the line (——) for an N_{BL}-N phase transition, the line (—·—·—·) for a P-N phase transition, the line (— — —) for a P-N_{BL} phase transition if $R > R_c \sim 0.22$ μm, and the line (–···–··–) for a P-N_{BL} phase transition if $R < R_c$.

Let us first concentrate our attention on the droplet radii above the critical value R_c. In the regime of weak surface interaction where $q < 0.39 \times 10^{-3}$ the transition temperature from the paranematic to the nematic phase decreases with decreasing droplet size because the influence of the director field distortions around the defect overcomes the ordering effect of the surface. At larger values of q, where $0.39 \times 10^{-3} < q < 0.96 \times 10^{-3}$ the surface ordering interaction dominates the disordering effect of the distortion. Therefore in this q range the transition temperature in smaller droplets is higher than in larger droplets (see Fig. 10). In the neighborhood of $q = q_{min} \sim 0.96 \times 10^{-3}$ the surface interaction becomes strong enough that it can also induce a separate N_{BL} phase before the transition into the nematic phase. The N to N_{BL} transition temperature only slightly changes with increasing surface interaction, but with increasing radius decreases and approaches the bulk transition temperature $\Delta T_{bulk} \sim 1.402$ K, because of the decreasing surface influence on the average molecule. The P-N_{BL} transition is nearly independent of R for $R > R_c$, but shifts to larger ΔT as q increases above q_{min}.

Below the critical radius $R = R_c$, where the N_{BL} phase cannot be distinguished from the nematic phase, the transition temperature to the paranematic phase strongly depends on the interaction q and radius R and is in most of this region suppressed far below T_{bulk}. The line of critical points q_{max} strongly depends on radius as well (Fig. 11).

Finally it should be mentioned that if the elastic constants are allowed to be different from each other (i.e., $L_2 \neq 0$) no qualitative changes are induced in the phase diagram. To show this we studied the spatial dependence of the order parameter in the neighborhood of the point defect where the behavior is believed to be very sensitive to the change of parameters. Taking into account Sheng's two-elastic-constant version[32] (L_1 and L_2) of the Landau–de Gennes expansion, the differential equation describing the spatial dependence of the order parameter reads

$$(\tfrac{3}{2}L_1+L_2)\left[\frac{\partial^2 S}{\partial r^2}+\frac{2}{r}\frac{\partial S}{\partial r}\right]-\left[\left[a(T-T_*)+\frac{18(L_1+\frac{1}{2}L_2)}{r^2}\right]S-bS^2+cS^3\right]+3L_2\frac{S}{r^2}=0\ . \tag{4}$$

Solutions for $S(r)$ deep in the nematic phase ($\Delta T=-5$ K) for the radius $R=0.1\ \mu\text{m}\sim 260\xi_0$ are presented in Fig. 12. Our single elastic constant $L_2=0$ is compared to the $L_2=L_1$ and $L_2=-L_1$ cases. Only minor differences in the behavior of the $S(r)$ function are observed.

V. CONCLUSIONS

We have studied phases with nematic-type ordering in a liquid crystal confined to a submicrometer droplet. Our discussion is limited to the case where liquid-crystal molecules orient on the average perpendicularly to the surface (strong homeotropic anchoring). In addition, the interfacial contribution to the free energy is assumed to be proportional to the degree of local orientational order. Although such a situation can be only partially realized in a real system the simplicity of the treatment and the relevance of the results for more complicated cases justify the use of our model. Strong perpendicular anchoring on the surface yields a radial direction of the director field and thus enables the use of a simple uniaxial (scalar) order parameter in the Landau–de Gennes expansion of the free energy.

The stable structures that result are influenced by the interplay of three phenomena: spontaneous nematic ordering, surface-induced nematic ordering, and depression of nematic ordering in regions of high elastic distortion. For large radii $R>0.22\ \mu\text{m}\sim 570\xi_0$ the transition between the nematic phase and the paranematic phase occurs directly only for $q<q_{\min}$ and $q>q_{\max}$. In the first case the paranematic phase exhibits weak surface-induced ordering while in the second case this ordering is high. In the intermediate range of q a separate phase with a relatively thick nematic boundary layer appears. In the limit of large droplet radii our results match with Sheng's predictions[19] for a nematic liquid crystal confined between parallel walls. For infinitely separated walls he obtained $q_{\min}\sim 1.04\times 10^{-3}$, $q_{\max}\sim 2.12\times 10^{-3}$. For the

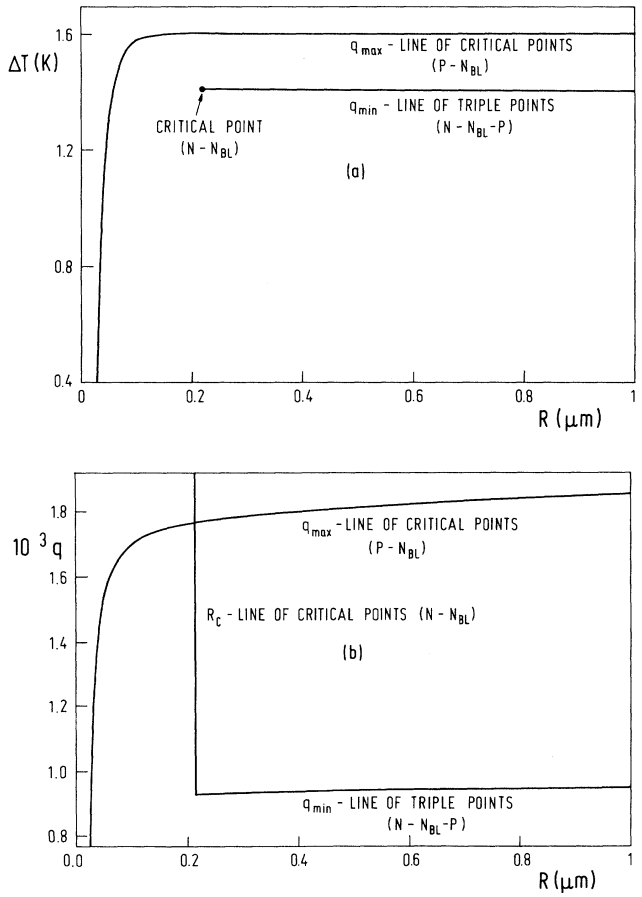

FIG. 11. Lines of critical points R_c and $q_{\max}$ together with the line of triple points $q_{\min}$ projected (a) on the temperature-radius plane and (b) on the surface interaction-radius plane.

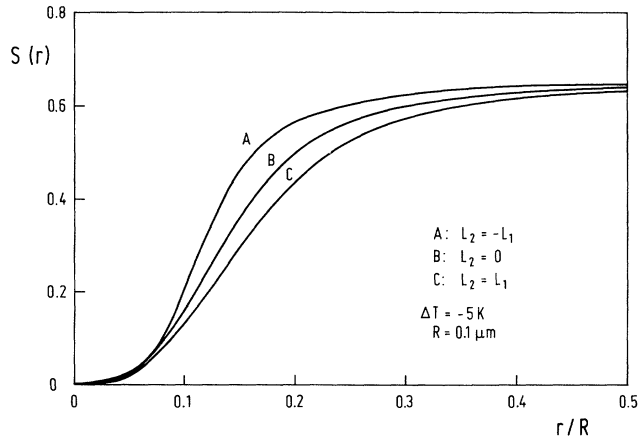

FIG. 12. The spatial variation of the order parameter near the point defect deep in nematic phase for three different sets of constants L_1 and L_2.

droplet radii $R=1\ \mu m \sim 2600\xi_0$, where the limit $R \to \infty$ is not yet realized, we got $q_{min} \sim 0.96 \times 10^{-3}$ and $q_{max} \sim 1.85 \times 10^{-3}$. It is obvious from our results that even in PDLC materials, where a high surface-to-volume ratio can be easily achieved, the surface transition will be very hard to detect experimentally since it exists only in a restricted range of surface interaction ($q_{min} < q < q_{max}$)—which is hard to control—and only in the interval 0.1 K above the transition to the nematic phase. Sheng's dependence of the transition temperature on the enclosure size qualitatively deviates from ours because the elastic distortion in the radial structure depresses the ordering within the droplet. For radii $R < R_c$, the nematic to paranematic transition occurs only at small q [$< q_{max}(R)$]. We have not studied in detail the region of small R and q since in this case the radial structure is certainly not stable in a real situation.

There are no experimental studies of small radial droplets, but our results are consistent with the studies of bipolar droplets. A deuterium NMR study[30] of the PDLC with bipolar droplets shows that $q > q_{min}$ and that the critical radius for the nematic to paranematic phase transition is between 0.35 and 0.035 μm, which is in agreement with a theoretical prediction 0.067 μm obtained in the limit of constant surface order parameter.[29] A much smaller critical radius in the bipolar case is a consequence of the minor effect of the elastic distortion on the ordering. There is a pronounced distortion around the poles but the central region below and above the equatorial plane is mostly not affected, while in the radial case the distortion in present everywhere. Therefore the bipolar case is expected to be somewhere in between the radial case where the effect of the distortion mainly determines the critical radius (0.22 μm) and the planar case where[19] the critical film thickness 0.02 μm is a consequence of the surface-induced ordering only.

There are several possible improvements of our simple model. The discussion of the effect of higher terms in the expansion of the homogeneous part of the Landau–de Gennes free energy[32] has shown that the behavior of the order parameter close to the defect is sensitive to the inclusion of such terms. The ordering in the surface layer is expected to be sensitive to inclusion of the surface terms with higher powers of $S(r)$ (Ref.32) and terms corresponding to K_{24} and K_{13} elastic constants.[34–36] The most important change in our model would be omission of the strong anchoring condition. Even in zero external field this results in a possible appearance of the axial configuration.[8,9] Unfortunately, a completely general treatment, which is much more complicated, should also include deformation-induced biaxiality.[37] Some of these improvements will be discussed in a subsequent paper[9] devoted to large nematic droplets with weak homeotropic anchoring on the surface.

ACKNOWLEDGMENTS

The authors acknowledge the support of the Natural Science Foundation under Solid State Chemistry Grant No. DMR88-17647.

[1]J. W. Doane, N. A. Vaz, B. G. Wu, and S. Žumer, Appl. Phys. Lett. **48**, 269 (1986).
[2]J. Fergason, SID Int. Symp. Dig. Tech. Pap. **16**, 68 (1985).
[3]J. W. Doane, A. Golemme, J. L. West, J. B. Whitehead, and B. G. Wu, Mol. Cryst. Liq. Cryst. **165**, 511 (1988).
[4]E. Dubois-Violette and O. Parodi, J. Phys. C **4**, 57 (1969).
[5]G. E. Volovik and O. D. Lavrentovich, Zh. Eksp. Teor. Fiz. **85**, 1997 (1983) [Sov. Phys.—JETP **58**, 1159 (1983)].
[6]S. Žumer and J. W. Doane, Phys. Rev. **34**, 3373 (1986).
[7]M. V. Kurik and O. D. Lavrentovich, Usp. Fiz. Nauk **154**, 381 (1988) [Sov. Phys.—Usp. **31**, 196 (1988)].
[8]J. H. Erdmann, S. Žumer, and J. W. Doane, Phys. Rev. Lett. **64**, 19 (1990).
[9]S. Kralj and S. Žumer (unpublished).
[10]R. D. Williams, J. Phys. A **19**, 3211 (1986).
[11]P. Drzaic, Mol. Cryst. Liq. Cryst. **154**, 289 (1988).
[12]S. Candau, P. LeRoy, and F. Debeauvais, Mol. Cryst. Liq. Cryst. **23**, 283 (1973).
[13]J. W. Doane, S. Žumer, and A. Golemme, in *Proceedings of the Tenth Ampere Summer School and Symposium, Portorož, 1988,* edited by R. Blinc, M. Vilfan, and J. Slak (J. Stefan Institute, Ljubljana, 1988), p. 189.
[14]A. Golemme, S. Žumer, J. W. Doane, and M. E. Neubert, Phys. Rev. A **37**, 559 (1988).
[15]S. Žumer, A Gollemme, and J. W. Doane, J. Opt. Soc. Am. **6**, 403 (1989).
[16]H. Schroder, J. Chem. Phys. **67**, 16 (1977).
[17]K. Miyano, J. Chem. Phys. **73**, 1994 (1980).
[18]D. W. Allender, G. L. Henderson, and D. L. Johnson, Phys. Rev. A. **24**, 1086 (1981).
[19]P. Sheng, Phys. Rev. A **3**, 1610 (1982).
[20]A. Poniewierski and T. J. Sluckin, Mol. Cryst. Liq. Cryst. **111**, 373 (1984).
[21]M. M. Telo da Gama, Mol. Cryst. **52**, 611 (1984).
[22]A. Mauger, G. Zribi, D. L. Mills, and J. Toner, Phys. Rev. Lett. **53**, 2485 (1984).
[23]T. J. Sluckin and A. Poniewierski, Phys. Rev. Lett. **55**, 2907 (1985).
[24]H. Hsiung, Th. Rasing, and Y. R. Shen, Phys. Rev. Lett. **57**, 3065 (1986).
[25]W. Chen, L. J. Martinez-Miranda, H. Hsiung, and Y. R. Shen, Phys. Rev. Lett. **62**, 1860 (1989).
[26]H. Yokoyama, S. Kobayashi, and H. Kamei, J. Appl. Phys. **61**, 4501 (1986).
[27]S. Žumer, M. Vilfan, and I. Vilfan, Liq. Cryst. **3**, 947 (1988).
[28]D. W. Allender and S. Žumer, Proc. SPIE **1080**, 18 (1989).
[29]I. Vilfan, M. Vilfan, and S. Žumer, Phys. Rev. A **40**, 4724 (1990).
[30]A. Golemme, S. Žumer, D. W. Allender, and J. W. Doane, Phys. Rev. Lett. **61**, 2937 (1988).
[31]De Gennes, The Physics of Liquid Crystals (Clarendon, Oxford, 1974).

[32]E. B. Priestley, P. J. Wojtowitz, and P. Sheng, *Introduction to Liquid Crystals* (Plenum, New York, 1974), p. 143.
[33]A. K. Sen and D. E. Sullivan, Phys. Rev. A **35**, 1391 (1987).
[34]J. Nehring and A. Saupe, J. Chem. Phys. **54**, 337 (1971).
[35]J. Nehring and A. Saupe, J. Chem. Phys. **56**, 5527 (1972).
[36]A. Strigazzi, Nouvo Cim. D **10**, 1335 (1988).
[37]K. Trebin and S. Trimper, Phys. Status Solidi B **118**, 267 (1983).